THE ANALYSIS OF A THERMAL STRESS STATE FOR INDUSTRIAL COMPOSITE PLATES

Tuğba Baytak
Civil Engineering Faculty, Istanbul Technical University
Maslak, 34469 Istanbul
Turkey

Osman Bulut
Civil Engineering Faculty, Istanbul Technical University
Maslak, 34469, Istanbul
Turkey

ABSTRACT
In industrial structures and machine elements, the composite plate elements produced by different materials are frequently encountered. Near the interface of the phases, some defects in different shapes and sizes caused by various factors can be observed. When thermal effects are not taken into account, important stress concentrations can occur around these defects. Therefore, the expected strength in design cannot be ensured during the service life. In this study, the state of thermal stress was analysed near the interface of materials with different coefficients of thermal expansion and around a cavity in the direction perpendicular to the plane of the interface. This analysis is performed by the stress freezing method and using the mechanical modeling of thermal stresses in three dimensional photoelasticity. The stress intensity factor at the tip of the cavity and thermal stress components perpendicular to the interface were obtained. Also, these results compared with the results obtained by the finite element analysis (FEM).
Keywords: Thermal stresses, photoelasticity, FEM.

1. INTRODUCTION
Composite materials used in many areas as structural elements are exposed to thermal effects during production and operation. Especially these materials are subjected to different types of mechanical or thermal effects during service. Due to these various effects, defects occur in different positions and in different geometries on the materials forming these plates [1, 2]. The components of the thermal stress are analytically obtained in literature depend on the boundary conditions and temperature change function [3, 4]. Studies on the analysis of stresses caused by mechanical effects in bimaterial elements are frequently encountered [5, 6, 7, 8]. Kenichi et al [9], evaluated the stress field around the crack on a glass plate under thermal loading. Although there are several works on mechanical loads in literature, studies on thermal stress state around defects occured by temperature distribution are few. In order to be able to safely design of the structures, the thermal stress distributions should be determined at the critical points.

In this study, thermal stress analysis of the plate made of two materials with different thermal expansions was performed. This plate has a cavity in the direction perpendicular to the plane of the interface. Such an application is seen in pressure vessels of nuclear reactors. These elements are produced by coating the steel body with stainless steel. When ΔT is the temperature difference, thermal stresses will occur as a result of different expansions of the materials. This problem is firstly studied experimentally by the method of photoelasticity. Numerical analysis was also performed using the finite element method to compare the experimental data in regions where analytical solution is not available. ABAQUS, finite element package program, was used for this analysis.

2. EXPERIMENTAL STUDY

In the experimental study, mechanical modeling method of photothermoelasticity was used [10]. For the experimental modeling of the prototype, the analogy of deformation defined in literature between two different thermoelasticity problems was used [4]. According to this analogy, the difference of thermal expansion occurring in two different cases are equalized. In the first case, a bimaterial plate, which represents the prototype produced by two materials having the same mechanical properties but different coefficients of thermal expansion, is subjected to the same temperature change. This was modeled by the second case which is a single material plate subjected to two different temperature changes on regions considered in the first case. According to this, the experimental model is made of the same two cylindrical plates. The material used is epoxy-based Araldite, which is a homogeneous, isotropic, linear-elastic and optical sensitive material.

The strain $\alpha\Delta T$, where α is the thermal expansion coefficient and ΔT is the temperature change of the element, was formed by mechanical modeling method of photoelasticity and these strains were fixed in the plate by freezing method of strain. To create the part on which the thermal effect occurs, a cylindrical specimen, made from the same material with the model, was used. This specimen was loaded by axial pressure in the furnace, which is suitable for the photoelastic examination. In the furnace, the sample was heated to the viscoelastic temperature of 155 °C in a special regime (Figure 1) of heating and the loading was applied at this temperature. Then, the sample was cooled to room temperature with the same regime, and the strains occurring at the viscoelastic temperature were fixed at room temperature.

From this specimen, a 3.9 mm thick plate was obtained by a precision cutting in order to create the thermal loaded part of the experimental model. Another plate having no mechanical effect was also produced. This part has the same diameter with the diameter of the other part on which the mechanical strains are frozen. These parts were glued to each other with a special process. Then, a cavity was formed in the model, which is perpendicular to the interface of the parts. This cavity was actually identified as one of the types of defects encountered in the industrial applications [1]. In this way, the experimental model formed by the combination of two cylindrical plates, was obtained (Fig. 2).
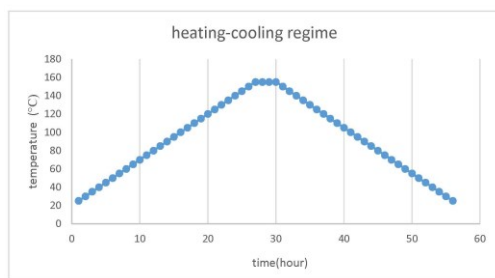

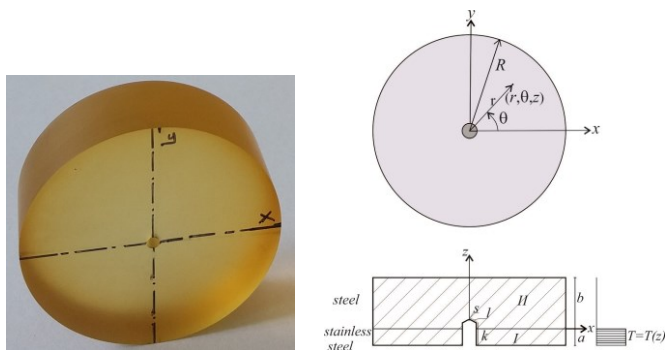Figure 1. Heating and cooling regime stress freezing method.

Figure 2. Experimental model of bimaterial plate.

Model dimensions are *a=3.90mm, b=12.60mm, R=25mm, k=1.60mm, l=1.44mm* and *s=0.33mm.* When the model was heated in the same heating regime up to the viscoelastic temperature, the strains on the first part, on which the thermal deformations were frozen, were released, but since the unloaded part did not allow this, a new stresses distribution occurred through the model. This stress distribution shows the thermal stress distribution in the prototype. Then, when the model was cooled to room temperature with the same special cooling regime, these deformations were fixed in the model. For thermal stresses analyses, the method of slicing of three-dimensional photoelasticity was used. A slice including the tip of the cavity with a thickness of 1.3 mm was cut out in the diameter direction. The distribution of thermal stresses were obtained on the slice along the direction given in Fig. 3.

Along this direction at each point, where the stress values was obtained, the number of fringe (*m*) was measured by a polarizing microscope and the thickness (*t*) of the slice through which light passes

was determined by a digital micrometer. In the model, optical sensitivity coefficient of the material is $\sigma_0^{1.0}$=0.233 N/(mm.fringe), $\alpha\Delta T$ =0.018, modulus of elasticity E=19.3 MPa and Poisson ratio ν= 0.49. Since the number of fringes at the points and the thickness values of the light passes through the slice were known, the difference of the principal stresses were calculated for all points by the related formula given in Eq. 1 [10].

$$|\sigma_1 - \sigma_2| = \sigma_0^{1.0}\frac{m}{t} \qquad \qquad \dots(1)$$

Measurements and calculations of dimensionless stresses are given in the Table 1. The calculated stresses in the fifth column were transformed into dimensionless stresses dividing them by $E\varepsilon = E\alpha\Delta T$ and the distribution of dimensionless stresses was plotted in Fig. 3.

Table 1. Measurements at the points determined on the slice and dimensionless stresses

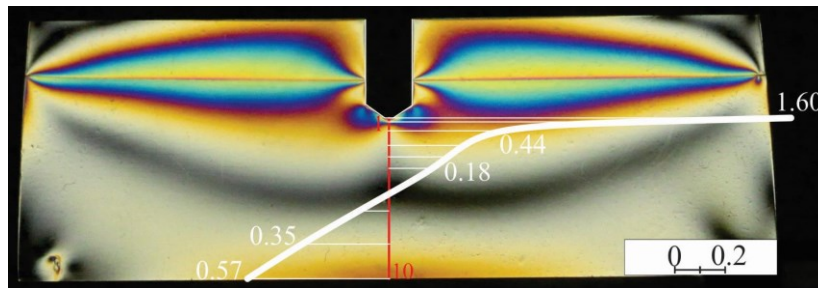| number	m (fringe)	$\sigma_0^{1.0}$ (N/mm.fringe)	d (mm)	$|\sigma_1 - \sigma_2|$ (MPa)	Dimensionless stress
1	2.295	0.233	0.96	0.56	1.60
2	1.426	0.233	0.97	0.34	0.98
3	0.636	0.233	0.97	0.15	0.44
4	0.515	0.233	0.97	0.12	0.36
5	0.353	0.233	0.97	0.08	0.24
6	0.263	0.233	1.00	0.06	0.18
7	0	0.233	1.04	0.00	0.00
8	0.203	0.233	1.10	0.04	0.12
9	0.577	0.233	1.12	0.12	0.35
10	0.941	0.233	1.11	0.20	0.57

Figure 3. Dimensionless stresses distribution

3. NUMERICAL ANALYSIS

Numerical analysis was performed using the finite element method to compare the experimental data in the model. ABAQUS, finite element package program, was used for this analysis. In the analysis, the mesh size was determined at 0.05 mm in the upper part of the axisymmetric model and 0.1 mm in the lower part. In both parts of the model, CAX4R (Four-node, bilinear, axially symmetrical quadrilateral, reduced integral and hourglass controlled) element type was used and the total number of elements was 57067. The distribution of the radial stress on the deflected finite element model is shown in Fig. 4. From the obtained results, the stress values in the relevant direction were compared with the results obtained here.

4. RESULTS AND DISCUSSION

Comparing the results from the experimental study with those from the finite element analysis, it was shown that the results have good agreement (Figure 5). In the models, the stress concentration occurs at the tip of cavity. The dimensionless stress measured at the tip of cavity formed in the experimental model is 1.60. Dimensionless stress is 1.62 obtained for the same point in the numerical solution. The rate of difference between these two was calculated as 1.25%.
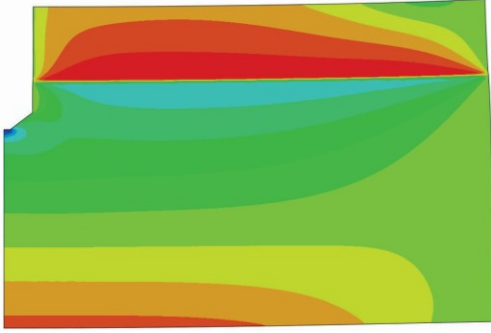
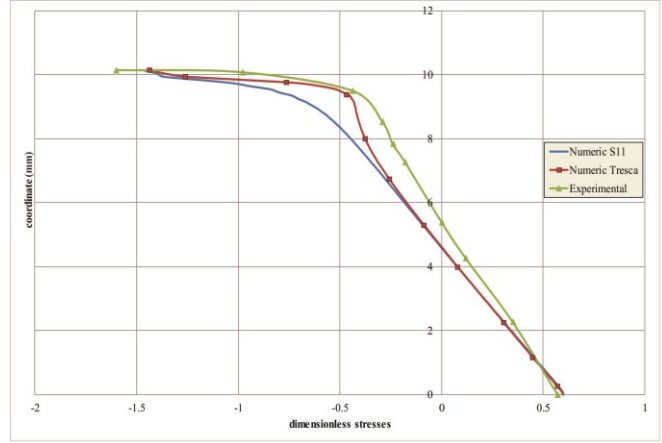*Figure 4. Finite element analysis model.*

Figure 5. Comparison of numerical and experimental dimensionless stress values in the model

In order to calculate the actual stress on a real application of this analysis, which is mentioned before, stainless steel and normal steel were respectively represented by the indices *1* and *2*, taking the related material coefficients as follows

$$\alpha_I = 16.10^{-6}1/{}^{\circ}C, \alpha_{II} = 16.10^{-6}1/{}^{\circ}C$$

$$E_n = E_I = E_{II} = 200 GPa, \nu_n = 0.3$$

Thermal stress value at the tip of the cavity was calculated as 208 MPa for the steel-stainless steel assembly as a prototype using the following formula [2]:

$$\sigma_n = \frac{1 - \nu_m E_n}{1 - \nu_n E_m} \kappa \sigma_m \tag{2}$$

where *n* and *m* represent the actual material and model respectively.

5. REFERENCES

[1] Abdulaliyev, Z., Ataoglu, S., Bulut, O. ve Kayali, E.S.: Three-dimensional stress state around corrosive cavities on pressure vessels, ASME Journal of Pressure Vessel Technology, 132(2), 2010.,

[2] Abdulaliyev, Z., Ataoglu, S. ve Guney, D.: Thermal stresses in butt-jointed thick plates from different materials, Welding Journal, 86(7), 201S–204S, 2007.,

[3] Timoshenko, S.P. ve Goodier, J.N.: Theory of Elasticity, Mc. Graw, London, 1970.,

[4] Boley, B.A. ve Weiner, J.H.: Theory of Thermal Stress, Dover Publications, New York, 1997.,

[5] S. Ataoglu, M. Tosun, T. Baytak, A. Donmez, O. Bulut, C. Ipek.: Stress Analysis and Microstructure of the Al2O3/Cu/MgB2 wires, Journal of Trends in the Development of Machinery and Associated Technology, Vol: 20 No: 1, pp. 57-60, 2016.,

[6] O. Bulut, A. Donmez, T. Baytak, M. Tosun, C. Ipek, S. Ataoglu, O. Cakiroglu, "Residual Stress and Microstructure of YSZ Buffer Layers for YBCO Coated Conductor", Journal of Trends in the Development of Machinery and Associated Technology, Vol: 20 No: 1, pp. 61-64, 2016.,

[7] Wu, D.F., Shang, L., Pu, Y. ve Wang, H.T.: Determination of stress intensity factor KIII for three-dimensional crack by using caustic method in combination with stress-freezing and stress releasing technique, Experimental Mechanics, 56(463-474),2016.,

[8] Kotousov, A. ve Wang, C.H.: Three-dimensional stress constraint in an elastic plate with a notch, International Journal of Solids and Structures, 39(16), 4311–4326, 2002.,

[9] Sakaue, K., Yoneyama, S., Kikuta, H. ve Takashi, M.: Evaluating crack tip stress field in a thin glass plate under thermal load, Engineering Fracture Mechanics, 75(5), 1015–1026, 2008.,

[10] Frocht, M.M.: Photoelasticity, Wiley, New York, 1941.